

# MrgprX2 regulates mast cell degranulation through PI3K/AKT and PLC $\gamma$ signaling in pseudo-allergic reactions

Fan Zhang<sup>a,b</sup>, Fang Hong<sup>a,b</sup>, Lu Wang<sup>a,c</sup>, Renjie Fu<sup>a</sup>, Jin Qi<sup>a,\*</sup>, Boyang Yu<sup>a,b,\*</sup>

<sup>a</sup> Jiangsu Key Laboratory for TCM Evaluation and Translational Research, School of Traditional Chinese Pharmacy, China Pharmaceutical University, Nanjing 21198, China

<sup>b</sup> Research Center for Traceability and Standardization of TCMs, China Pharmaceutical University, Nanjing 21198, China

<sup>c</sup> Nanjing Hospital of Chinese Medicine Affiliated to Nanjing University of Chinese Medicine, China

## ARTICLE INFO

### Keywords:

Pseudo-allergic reactions  
Mast cell  
MrgprX2  
PI3K/AKT  
PLC $\gamma$

## ABSTRACT

The G protein-coupled receptor MrgprX2 in mast cells is known to be a crucial receptor for pseudo-allergic reactions. MrgprX2 activation leads to elevated intracellular calcium levels and mast cell degranulation, but the underlying mechanism remains to be elucidated. Herein, we investigated the role of the phosphatidylinositol 3 kinase (PI3K)/serum-threonine kinase (AKT) signaling pathway and phospholipase C gamma (PLC $\gamma$ ) in mast cell degranulation mediated by MrgprX2 in LAD2 human-derived mast cells. The results showed that phosphorylated AKT (p-AKT) and PLC $\gamma$  up-regulation were accompanied by an increase in intracellular calcium following activation of MrgprX2 by Compound 48/80, an inducer of mast cell degranulation. In contrast, p-AKT and PLC $\gamma$  were down-regulated and intracellular calcium levels decreased after MrgprX2 knockdown. Mast cell degranulation was clearly suppressed; however, inhibiting PI3K and PLC $\gamma$  phosphorylation did not influence MrgprX2 expression. The increase in calcium concentration was suppressed and mast cell degranulation was weakened. Furthermore, by inhibiting PI3K and PLC $\gamma$  phosphorylation in animals, the allergic symptoms caused by C48/80 were obviously reduced. We deduced that during the mast cell degranulation observed in pseudoallergic reactions, MrgprX2 regulated intracellular calcium levels via the PI3K/AKT and PLC $\gamma$  pathways.

## 1. Introduction

Pseudo-allergic reactions (PARs), also called anaphylactoid reactions, occur in the absence of a specific antigen, and are frequently observed clinically [5,23,28]. Although PARs are common, scientists do not have a deep understanding of their underlying mechanisms, which leads to difficulties in clinical management and treatment.

PARs and allergic reactions have similar symptoms, such as dilation of capillaries, increased vascular permeability, contraction of smooth muscle, and increased secretion of mucus glands [9]. However, unlike allergic reactions, PARs occur independently of IgE activation [6].

Compound 48/80 (C48/80), a condensation product of N-methyl p-methoxyphenethylamine and formaldehyde, is commonly used in PAR research as it can promote mast cells degranulation [10]. Research on the PAR was very limited until 2015, when the breakthrough study by McNeil et al. determined that MrgprX2, a G protein-coupled receptor on mast cells, was the key receptor in the occurrence of PARs [14]. When the Mrgprb2, a homologous MrgprX2 receptor in mice, was

conditionally knocked out, C48/80-induced PARs symptoms were greatly weakened or even disappeared *in vivo*. Furthermore, C48/80-induced mast cells degranulation was significantly reduced following knockdown of MrgprX2 in LAD2 cells *in vitro*.

As a second messenger, calcium ions (Ca<sup>2+</sup>) are involved in various physiological processes [3]. In PARs, mast cell degranulation is mainly dependent on increased intracellular Ca<sup>2+</sup> levels [25]. Studies have reported that PLC $\gamma$  activation can promote inositol triphosphate (IP3) production, which promotes Ca<sup>2+</sup> release from the Ca<sup>2+</sup> reservoir of the endoplasmic reticulum, mediated by IgE-mast cell degranulation [15,32]. Furthermore, the PI3K/AKT signaling pathway also plays a crucial role IgE-induced mast cell degranulation by regulating intracellular Ca<sup>2+</sup> levels [30,31]. When the cytosolic Ca<sup>2+</sup> concentration increases, the Ca<sup>2+</sup> and calmodulin (CaM) complex induces a conformation change which in turn activates the CaM protein kinase (CaMK) [19]. CaMK activates tubulin and myosin light chains to participate in the transport and orientation of vesicles [21]. Histamine,  $\beta$ -hexosaminidase and tryptase are stored in vesicles and released accompany

\* Corresponding authors at: China Pharmaceutical University, Nanjing 21198, China.

E-mail addresses: [qijin2006@163.com](mailto:qijin2006@163.com) (J. Qi), [boyangyu59@163.com](mailto:boyangyu59@163.com) (B. Yu).

<https://doi.org/10.1016/j.intimp.2021.108389>

Received 10 August 2021; Received in revised form 27 October 2021; Accepted 9 November 2021

Available online 15 December 2021

1567-5769/© 2021 Elsevier B.V. All rights reserved.

with mast cell degranulation. Thus, the release of  $\beta$ -hexosaminidase is often used as indicator of mast cell degranulation [13].

Herein, we focused on the mechanism involved in mast cell degranulation caused by MrgprX2 activation in PARs. We attempted to determine whether activated MrgprX2 influences changes in intracellular  $\text{Ca}^{2+}$  levels through the PI3K/AKT pathway and PLC $\gamma$  to ultimately induce mast cell degranulation.

## 2. Materials and methods

### 2.1. Reagents

Compound 48/80 (C2313) and BAPTA-AM (A1076) were purchased from Sigma-Aldrich (America). Bicinchoninic acid (BCA) assay kit (P0012), Fluo-4 AM (S1060) and LY294002 (S1737) were purchased from Beyotime Biotechnology (China). U73122, an inhibitor of PLC $\gamma$ , was obtained from MedChemExpress (HY-13419, America). Evens blue was got from Solarbio (E8010, America). Stempro-34 SFM medium was purchased from Gibco (10639011, USA). Recombinant human stem cell factor (rhSCF) was obtained from Peprotech (GMP300-07, USA). Opti-MEM medium was purchased from Gibco (11058021, USA). HiPerFect Transfection Reagent was got from QIAGEN (301704, German). High sensitivity ECL chemiluminescence detection kit (E412, Vazyme Biotech, Nanjing, China).

### 2.2. Cell culture

Laboratory of allergic disease 2 (LAD2) cells were gifted by Dr. Kirshenbaum of the National Institute of Allergy and Infectious Diseases/National Institutes of Health. The cells were suspended in T25 cell culture flasks without TC treatment (5 mL/cell culture flask). Half of fresh complete medium was replaced every 7 days and perform cell passage every 10–14 days. Stem Pro-34 Nutrient Supplement, penicillin (100 IU/mL), streptomycin (100  $\mu$ g/mL) Glutamine (2 mM) and rhSCF (100 ng/mL) were added in cell medium.

### 2.3. Determination of $\beta$ -hexosaminidase

LAD2 cells in logarithmic growth phase were collected, centrifuged at 800 rpm/min for 4 min. The supernatant was discarded, and a certain amount of HEPES buffer was added to resuspend. The cells were seeded in a 96-well plate and assimilated in a 37 °C, 5% CO $_2$  incubator for 1 h. Then each group was given HEPES buffer or corresponding test solution for 30 min. After that, except the blank group, which was given HEPES buffer, the rest of the groups were given C48/80 stimulation.

Referred to literature [14], after incubated with C48/80 for 30 min, 50  $\mu$ L cell supernatant was transferred to a new 96-well plate and 50  $\mu$ L reaction substrate was added (4-nitrobenzene-N-acetyl- $\beta$ -D-amino-hexose in citric acid/Sodium citrate buffer, 0.1 mM, pH 4.5). Incubated at 37 °C for 1 h, then 150  $\mu$ L of stop solution (Na $_2$ CO $_3$ /NaHCO $_3$  buffer, pH 11.0) was added, and the absorbance was measured at 405 nm to obtain the Optical density (OD) value of the supernatant. Besides, at the same time, the supernatant of the original 96-well plate was discarded, and cell lysate (0.3% TritonX-100 in PBS buffer) was added to each well, and incubated at 37 °C for 40 min. 50  $\mu$ L of the cell lysate was transferred to a new 96-well plate and 50  $\mu$ L of the reaction substrate was added each well. After incubating at 37 °C for 1 h, 150  $\mu$ L of stop solution was added, and the absorbance was measured at 405 nm to obtain the OD value of the lysate. Calculate  $\beta$ -hexosaminidase release rate using the following formula:

$$\beta\text{-hexosaminidase release rate}(\%) = \frac{OD(\text{supernatant})}{OD(\text{supernatant}) + OD(\text{lysate})} \times 100\%$$

### 2.4. Transfection

LAD2 cells were collected and centrifuged at 800 rpm/min for 4 min, then resuspend with Stempro-34 medium without double antibodies, nutrient solution and SCF. After that, LAD2 cells were seeded in a 24-well plate. 24 h later, 4.5  $\mu$ L transfection reagent was added into 50  $\mu$ L Opti-MEM medium. 0.9  $\mu$ L of siRNA stock solution was added into 50  $\mu$ L Opti-MEM medium to final concentration at 30 nM. The siRNA sequences were as follow: siRNA-MrgprX2: Forward-5'-GUACAACAGUGAAUGGAAATT-3', Reverse-5'-UUUCCAUUCACUGUUGUACTT-3'; siRNA-Negative control: Forward-5'-UUCUCCGACGUGUCACGUTT-3', Reverse-5'-ACGUGACACGUUC-GGAGAATT-3'. The diluted transfection reagent and siRNA solution were mixed gently, and added into 24-well plate as 100  $\mu$ L/well. After 6 h, the medium was replaced with Stempro-34 complete medium without double antibodies, then the incubating continued for 48 h.

### 2.5. Intracellular $\text{Ca}^{2+}$ concentration determination

LAD2 cells were incubated with the test solution 30 min in advance. The medium was discard, and then the Fluo-4 AM was added (2  $\mu$ M, 60  $\mu$ L/well, 96-well plate). Then the cell plate was put into the incubator for 60 min. 140  $\mu$ L Locke's buffer solution was added to each well so that the volume of the liquid in every well was 200  $\mu$ L. Then 150  $\mu$ L solution was discard and 150  $\mu$ L fresh Locke's buffer was added, repeating 4 times. Finally, 150  $\mu$ L solution was discarded again, then 100  $\mu$ L of Locke's buffer was added to make the volume to be 150  $\mu$ L per well. After that, cell plate was placed in the READ position of a fluorescent imaging plate reader (FLIPRTetra®; Molecular Devices, Sunnyvale, CA) and stabilize for 5 min. The prepared test solution was vortex and added to the corresponding position on the V bottom plate. The background fluorescence value of the cell plate was between 500 and 600. Then the intracellular  $\text{Ca}^{2+}$  concentration was measured.

### 2.6. Western blotting

LAD2 Cells were lysed in ice-cold radioimmunoprecipitation assay (RIPA) buffer (within 1 mM phenylmethylsulfonyl fluoride). The protein concentrations were determined by BCA assay kit. Proteins were separated by 10% sodium dodecyl sulphate-polyacrylamide gel electrophoresis and transferred onto PVDF membranes. The membranes were blocked with blocking buffer and incubated overnight with primary antibodies against t-AKT (1:1000, ab8805), p-AKT (1:1000, ab81283), PI3K (1:1000, ab32089), MrgprX2 (1:800, ab237047), PLC $\gamma$  (1:1000, ab52200) (Abcam, Cambridge, UK) and GAPDH (AP0063, Bioworld Technology, USA) at 4°C, respectively. Membranes were then probed with peroxidase-conjugated secondary antibody HRP-anti-rabbit (1:8000, BS13278) or HRP-anti-mouse (1:8000, BS12478) (Bioworld Technology, USA) at 25°C for 2 h. The antigen-antibody complexes were then detected with high sensitivity ECL chemiluminescence detection kit, visualized using a ChemiDoc MP system (Bio-Rad, Hercules, USA), and analyzed using Image Lab™ Software (version 4.1, Bio-Rad).

### 2.7. Animals

Healthy C57BL/6 mice (male, weighing 25 g) were purchased from the Center of Experimental Animals of Yangzhou University (Jiangsu, China). Animal quality certificate number: SCXK 2017-0007. The experimental animals were kept in an independent breeding room (23  $\pm$  1°C) on a 12 h light/dark cycle. Mice were provided with adequate food and water.

### 2.8. Local PARs in mice

Referred to literature [14], after anesthetized, the mice were injected

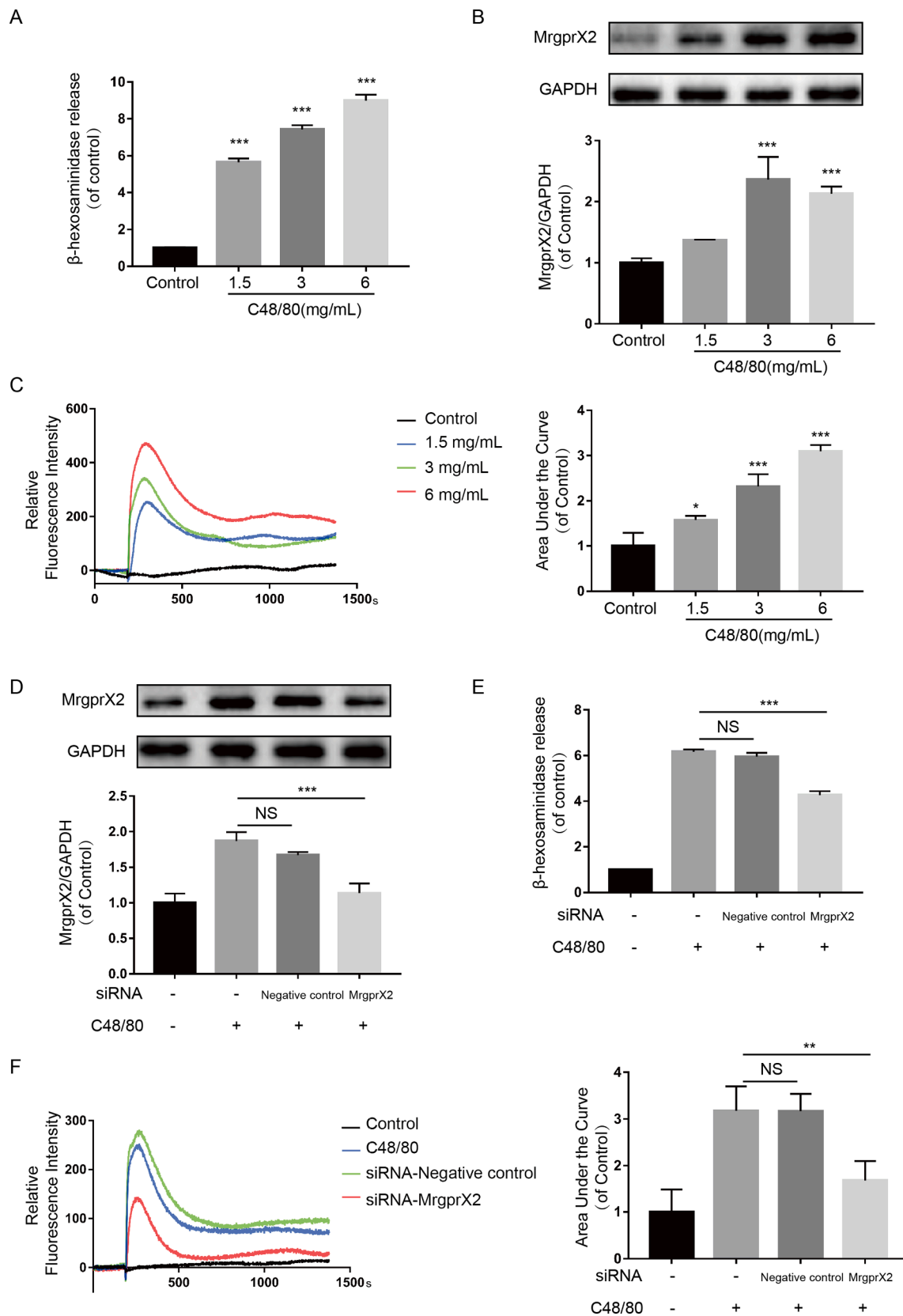


**Fig. 1.** MrgprX2 is essential for C48/80-induced LAD2 cell degranulation. A) β-hexosaminidase release from LAD2 cells induced by C48/80; B) Changes in MrgprX2 expression following LAD2 cell degranulation; C) C48/80 induced intracellular Ca<sup>2+</sup> concentration is elevated in LAD2 cells; D) MrgprX2 expression is reduced following transfection with MrgprX2-siRNA; E) Knockdown MrgprX2 weakens β-hexosaminidase release from LAD2 cells induced by C48/80; F) knockdown MrgprX2 inhibits intracellular Ca<sup>2+</sup> increase induced by C48/80. Except where noted, C48/80 was used at 6 mg/mL. All experiments were repeated in triplicate. Data are presented as the mean ± SD, and were analyzed using analysis of variance (ANOVA). Two-tailed tests were used for comparisons between two groups. Differences were considered significant at \**p* < 0.05, \*\**p* < 0.01, \*\*\**p* < 0.001 with Control. NS: not significant (*p* > 0.05). *n* = 3.

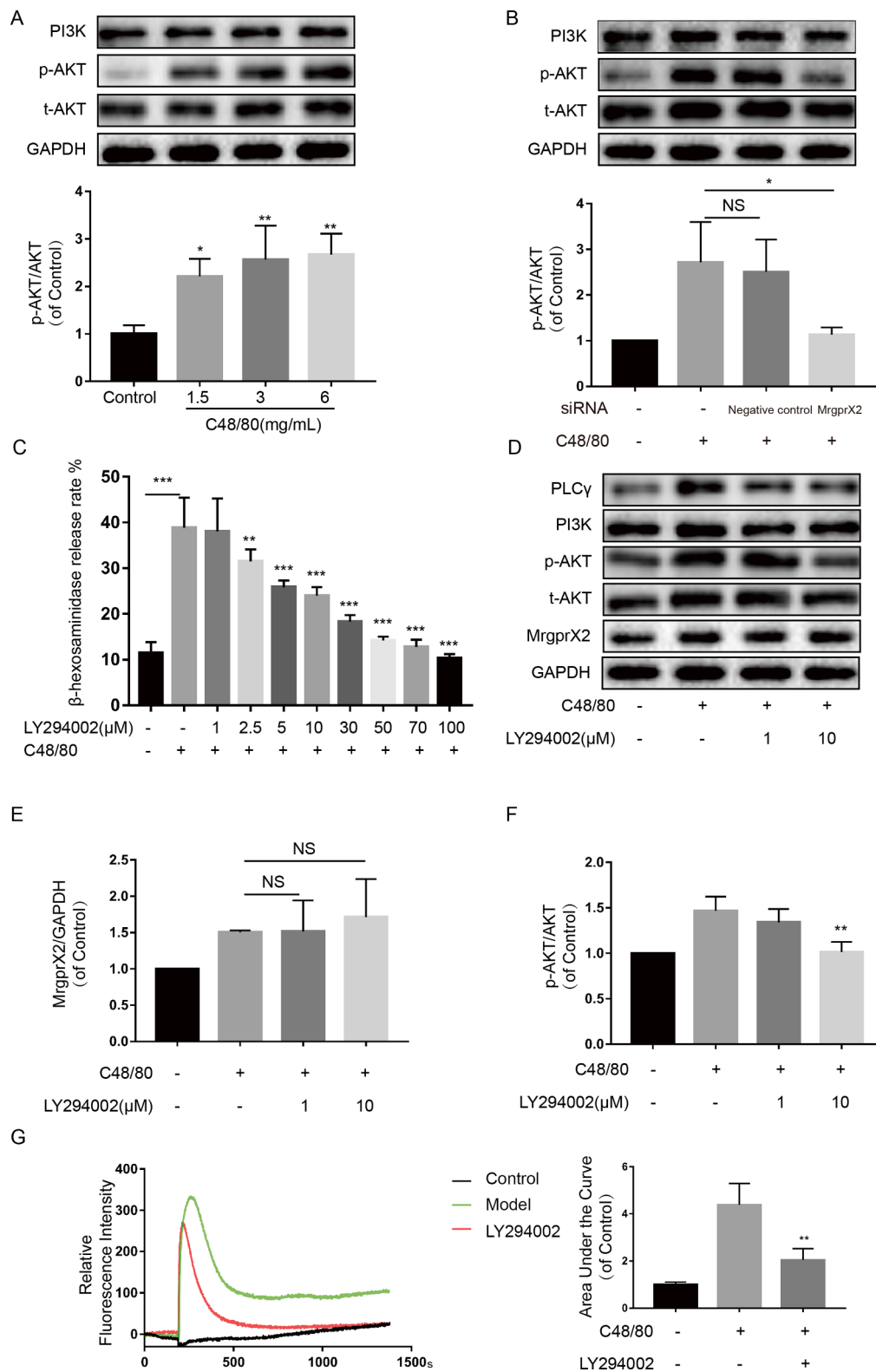


**Fig. 2.** PI3K/AKT acts downstream of MrgprX2 and is involved in LAD2 cell degranulation. A) AKT phosphorylation induced by C48/80; B) Knockdown MrgprX2 is inhibited C48/80-induced AKT phosphorylation; C) LY294002 dose-dependently reduced β-hexosaminidase release induced by C48/80; D) Effects of LY294002 on expression of p-AKT, t-AKT, PI3K, MrgprX2 and PLCγ; E) Effects of LY294002 on MrgprX2 expression; F) LY294002 inhibits AKT phosphorylation induced by C48/80; G) LY294002 (10 μM) inhibits the increase in intracellular Ca<sup>2+</sup> induced by C48/80. Except where noted, C48/80 was used at 6 mg/mL. p-AKT: phosphorylated AKT. t-AKT: total AKT. Experiments were repeated in triplicate. Data are presented as the mean ± SD and were analyzed using analysis of variance (ANOVA). Two-tailed tests were used for comparisons between two groups. Differences were considered significant at \**p* < 0.05, \*\**p* < 0.01 with Control, \*\*\**p* < 0.001 with Model. NS: not significant (*p* > 0.05). *n* = 3.

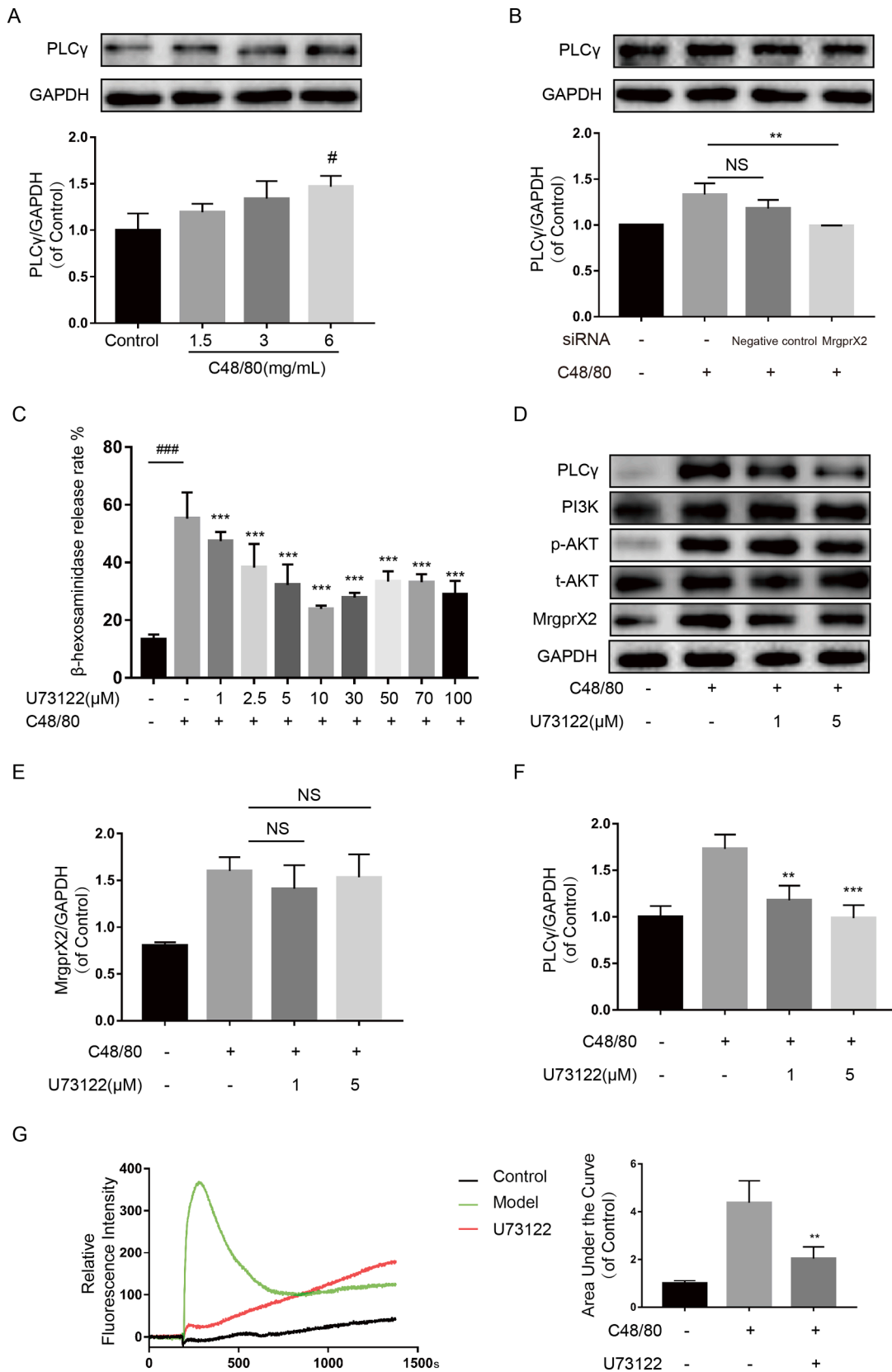


**Fig. 3.** PLCγ acts as a downstream of MrgprX2 and is involved in LAD2 cell degranulation. A) PLCγ expression induced by C48/80; B) Knockdown MrgprX2 inhibited PLCγ expression induced by C48/80; C) U73122 reduced β-hexosaminidase release induced by C48/80; D) Effect of U73122 on expression of PLCγ, PI3K, p-AKT, AKT, and MrgprX2; E) effect of U73122 on MrgprX2 expression; F) U73122 inhibits PLCγ expression induced by C48/80; G) U73122 (5 μM) inhibits intracellular Ca<sup>2+</sup> increase induced by C48/80. Except where noted, C48/80 was used at 6 mg/mL. Experiments were repeated in triplicate. Data are presented as the mean ± SD. and were statistically analyzed using analysis of variance (ANOVA). Two-tailed tests were used for comparisons between two groups. Differences were considered significant at <sup>#</sup>*p* < 0.05, <sup>###</sup>*p* < 0.001 with Control, <sup>\*\*</sup>*p* < 0.01, <sup>\*\*\*</sup>*p* < 0.001 with Model. NS: not significant (*p* > 0.05). *n* = 3.

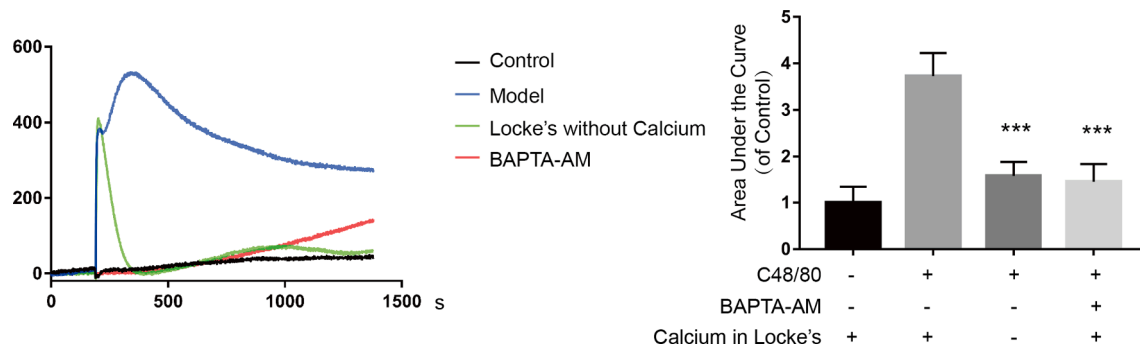


**Fig. 4.** Changes in intracellular  $\text{Ca}^{2+}$  concentration in LAD2 cells induced by C48/80. Intracellular  $\text{Ca}^{2+}$  concentration change in  $\text{Ca}^{2+}$ -free Locke's or with the use of the chelator BAPTA-AM (10  $\mu\text{M}$ ). C48/80 was used at 6 mg/mL. Experiments were repeated in triplicate. Data are presented as the mean  $\pm$  SD, and were analyzed using analysis of variance (ANOVA). Differences were considered significant at \*\*\*  $p < 0.001$  with Model.  $n = 3$ .

with 0.4% Evans Blue-saline solution (0.15 mL each) from tail vein. 5 min later, the thickness of the left and right hind paws was measured and recorded. Then, 5  $\mu\text{L}$  saline was injected into the left foot as self-control, and 5  $\mu\text{L}$  test solution was injected into the right foot. During the whole Local PARs experiments, the C48/80 was used at 10  $\mu\text{g}/\text{mL}$ . The LY294002 was used at 3 doses: low (3.2  $\mu\text{M}$ ), middle (6.4  $\mu\text{M}$ ) and high (12.8  $\mu\text{M}$ ). Similar, the U73122 was used at 3 doses: low (1  $\mu\text{M}$ ), middle (2  $\mu\text{M}$ ) and high (4  $\mu\text{M}$ ). After 15 min, the thickness of the paws was measured again. Then, the mice were sacrificed, the paws were photographed, and the left and right paws were weighed, dried at 60  $^{\circ}\text{C}$  for 24 h, then weighed again. Each dried paw was cut and soaked into 1 mL formamide, incubated at 37  $^{\circ}\text{C}$  for 72 h, and then centrifuged at 12,000 rpm for 15 min. Finally, 200  $\mu\text{L}$  of supernatant was pipetted and the absorbance was measured at a wavelength of 620 nm.

## 2.9. Systemic PARs in mice

Referred to literature [8,27], 0.4% Evans Blue solution was injected into mice from tail vein (0.25 mL each). Along the whole systemic PARs experiments, the C48/80 was used at 2 mg/mL. The LY294002 was used at 3 doses: low (32  $\mu\text{M}$ ), middle (64  $\mu\text{M}$ ) and high (128  $\mu\text{M}$ ). Similar, the U73122 was used at 3 doses: low (10  $\mu\text{M}$ ), middle (20  $\mu\text{M}$ ) and high (40  $\mu\text{M}$ ). After 15 min, the mice were sacrificed, and the ears and lung tissues of the mice were removed. The ears were weighted and immersed in 1 mL formamide solution and incubated at 37  $^{\circ}\text{C}$  for 72 h, then centrifuged at 12,000 rpm for 15 min. After that, 200  $\mu\text{L}$  of the supernatant was pipetted and the absorbance was measured at a wavelength of 620 nm. The lung tissue was rinsed with physiological saline 3 times and weighted, then dried at 60  $^{\circ}\text{C}$  for 24 h and weighing. Each dried lung tissue was immersed in 4 mL formamide and incubated at 37  $^{\circ}\text{C}$  for 72 h, then centrifuged at 12,000 rpm for 15 min. Finally, 200  $\mu\text{L}$  of supernatant was pipetted and the absorbance was measured at a wavelength of 620 nm.

## 2.10. Data analysis

All statistical analyses were performed using the Prism program (Version 7, GraphPad, San Diego, CA). In those cases in which the data tested positive for normal distribution (by using the Kolmogorov-Smirnov test), we conducted Unpaired Student's  $t$ -test for 2 groups and one-way analysis of variance (ANOVA) for more than 2 groups. In those cases in which the data were not normally distributed, the Kruskal-Wallis test was applied. Association of parameters was determined by the Pearson product-moment correlation for parametric data or by Spearman correlation for nonparametric data. Data are presented as means plus or minus standard deviation (SD).  $p < 0.05$  was accepted as statistical significance.

## 3. Results

### 3.1. MrgprX2 is crucial in LAD2 cell degranulation

C48/80 stimulation significantly increased the release of  $\beta$ -hexosaminidase from LAD2 (Fig. 1A). Similarly, the expression of MrgprX2 was up-regulated (Fig. 1B) and intracellular  $\text{Ca}^{2+}$  concentration was also markedly increased (Fig. 1C). However, when the expression of MrgprX2 was knocked down, C48/80-induced  $\beta$ -hexosaminidase release was significantly weakened (Fig. 1D, E) and the increase in intracellular  $\text{Ca}^{2+}$  concentration was also inhibited in LAD2 cells (Fig. 1F). This suggests that the MrgprX2-mediated mast cell degranulation reaction relied on increased intracellular  $\text{Ca}^{2+}$  levels.

### 3.2. PI3K/AKT was activated downstream of MrgprX2 during PARs

In LAD2 cells, AKT phosphorylation was significantly increased after C48/80 stimulation (Fig. 2A), but reduced along with MrgprX2 knock-down (Fig. 2B). Interestingly, in the presence of LY294002, a potent inhibitor of PI3K, C48/80 did not induce either an increase in intracellular  $\text{Ca}^{2+}$  concentration or mast cell degranulation (Fig. 2C, G). Furthermore, AKT phosphorylation was also markedly inhibited, but without no significant change in MrgprX2 expression (Fig. 2E, F). This indicated that PI3K/AKT could be a downstream signal of MrgprX2 during PARs.

### 3.3. PLC $\gamma$ is activated downstream of MrgprX2 during PARs

PLC $\gamma$  expression was noticeably up-regulated after C48/80 stimulation (Fig. 3A), but was reduced following knockdown of MrgprX2 (Fig. 3B). In the presence of U73122, a PLC $\gamma$  inhibitor, C48/80 failed to induce an increase in intracellular  $\text{Ca}^{2+}$  concentration and mast cell degranulation (Fig. 3C, G). Furthermore, PLC $\gamma$  expression was markedly reduced but did not change MrgprX2 expression (Fig. 3D-F). This suggested that PLC $\gamma$  might be a downstream target of MrgprX2, and activation of MrgprX2 induces PLC $\gamma$  activation and increase expression of PLC.

### 3.4. Calcium fluctuations in mast cells induced by MrgprX2

In order to explore the role of MrgprX2 in the regulation of intracellular  $\text{Ca}^{2+}$  in mast cells following stimulation by C48/80, we used  $\text{Ca}^{2+}$ -free Locke's medium and the  $\text{Ca}^{2+}$  chelator BAPTA-AM, to pre-chelate the intracellular  $\text{Ca}^{2+}$  pool. Interestingly, in  $\text{Ca}^{2+}$ -free Locke's medium, C48/80 caused a rapid increase in intracellular  $\text{Ca}^{2+}$  in LAD2 cells and the peak was reached quickly, which was followed by a rapid decrease in intracellular  $\text{Ca}^{2+}$  levels. However, when cells were pre-treated with BAPTA-AM, which depleted the intracellular  $\text{Ca}^{2+}$  pool, C48/80 did not cause a rapid increase in intracellular  $\text{Ca}^{2+}$  levels in

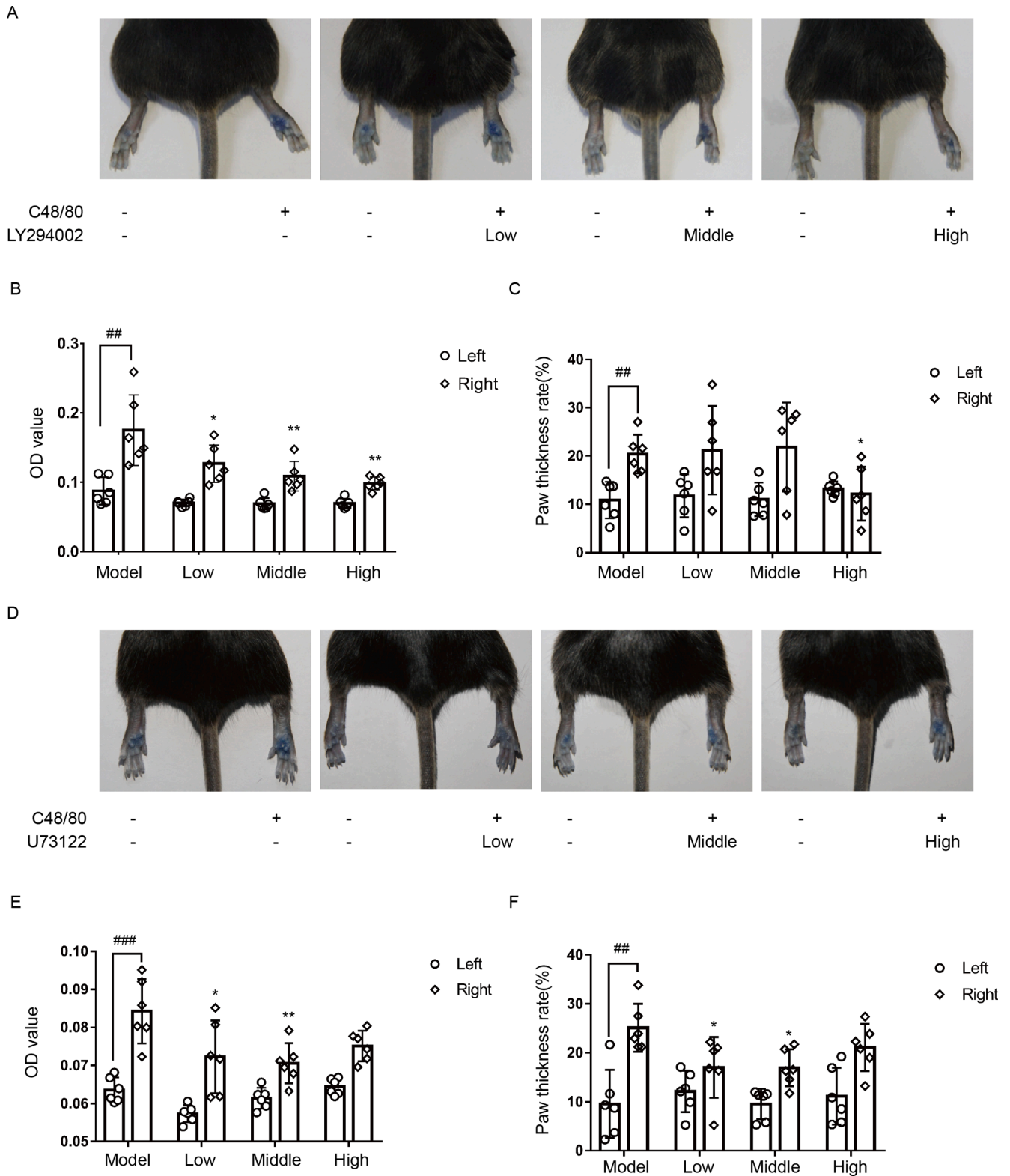


**Fig. 5.** Treatment with the PI3K/AKT inhibitor (LY294002) or PLC $\gamma$  inhibitor (U73122) suppress the pseudoallergic reactions (PARs) *in vivo*. A, D) representative images of Evans blue stained extravasation; B, E) Quantification of Evans blue leakage into the paw tissue from vessels; C, F) Changes in paw thickness. OD: Optical density. Data are presented as the mean  $\pm$  SD. and were analyzed using analysis of variance (ANOVA). Two-tailed tests were used for comparisons between two groups. Differences were considered significant at ##  $p < 0.01$ , ###  $p < 0.001$  with self-control, \*  $p < 0.05$ , \*\*  $p < 0.01$  with Model. NS: not significant ( $p > 0.05$ ). n = 6.

LAD2 cells (Fig. 4). In comparison, treatment with LY294002, an inhibitor of PI3K, intracellular Ca<sup>2+</sup> levels in LAD2 exerted the same effects on cells culturing cells in the Ca<sup>2+</sup>-free buffer, while pretreatment with U73122, an inhibitor of PLC $\gamma$ , produced similar effects as chelating

the intracellular Ca<sup>2+</sup> pool with BAPTA-AM.

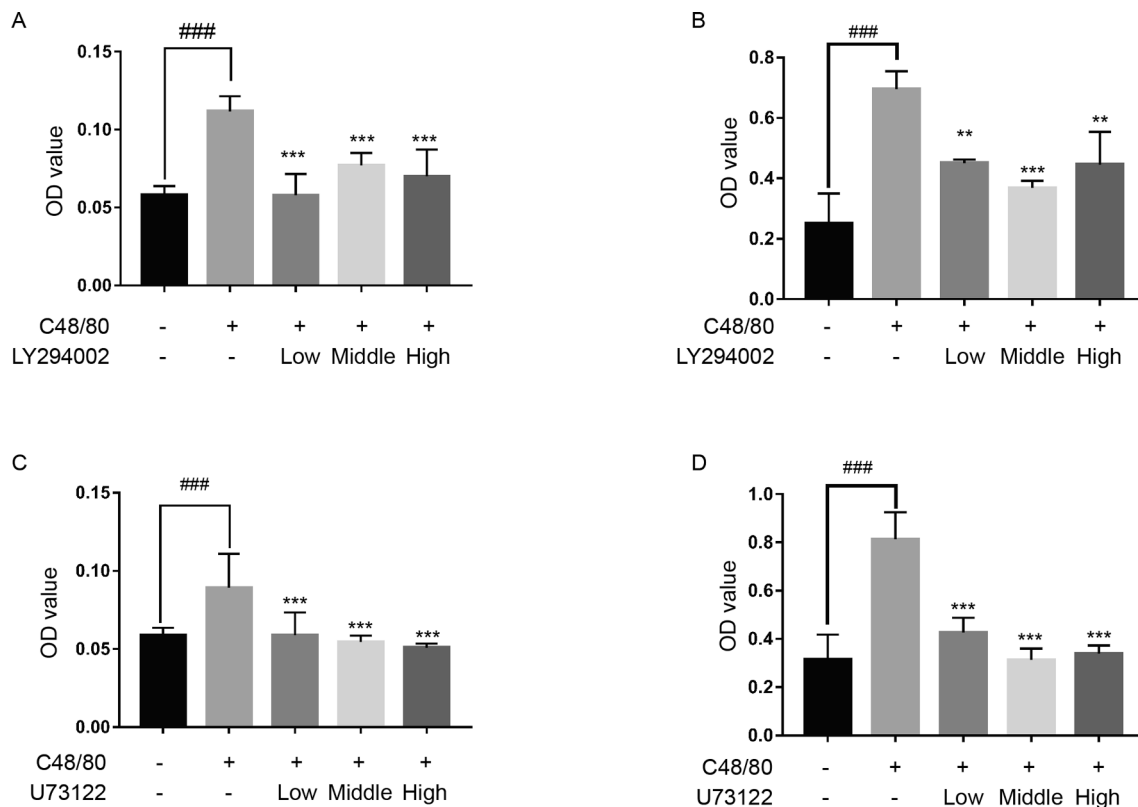


**Fig. 6.** Systemic administration of PI3K/AKT inhibitor (LY294002) or PLC $\gamma$  inhibitor (U73122) can suppress pseudoallergic reactions (PARs) *in vivo*. A, C) Quantification of Evans blue leakage into the ear from vessels following treatment with different concentrations of LY294002 or U73122; B), D) Quantification of Evans blue leakage into the lung following treatment with different concentrations of LY294002 or U73122. OD: Optical density. Data are presented as the mean  $\pm$  SD. and were statistically analyzed using analysis of variance (ANOVA). Two-tailed tests were used for comparisons between two groups. Differences were considered significant at  $###p < 0.001$  with Control,  $**p < 0.01$ ,  $***p < 0.001$  with Model.  $n = 6$ .

### 3.5. Role of PI3K/AKT and PLC $\gamma$ in PAR activity *in vivo*

The role of PI3K/AKT and PLC $\gamma$  in PARs was further verified *in vivo*. It is known that when the vascular permeability increases, the integrity of the vascular wall is destroyed, thus the substances extravasate from the blood vessel. We used absorbance of Evans Blue in the exudate to reflect the status of vascular leakage. Animal experiments were divided into local experiments and systemic experiments. As shown in Fig. 5, an intraplantar injection of LY294002 and U73122 inhibited Evans blue leakage from the local blood vessel and reduced paw swelling. Furthermore, a tail vein injection of LY294002 and U73122 reduced Evans blue leakage in the ears and lungs of mice. This suggested that both agents inhibited the increase in systemic vascular permeability (Fig. 6).

## 4. Discussion

Epidemiological studies have shown that approximately 20% of individuals worldwide experience allergic diseases, which has become an important public health concern worldwide [24]. Mast cell, as a tissue-resident immune cell, plays an important role in allergic diseases [17]. Clinically, drugs inducing mast cell degranulation is a result of MrgprX2 activation rather than IgE-mediated activation, such as muscle relaxants, opioids, Icatibant, fluoroquinolones and several Chinese herbal ingredients [11]. MrgprX2, is an orphan receptor, whose specific ligand is unknown. Therefore, exploring and discovering downstream pathways of MrgprX2 is promising for the development of drugs for the PARs treatment.

PI3K participates in a variety of cellular processes, including apoptosis, transcription, translation, metabolism, angiogenesis, and cell

cycle regulation [7]. Abnormal activation of the PI3K/Akt pathway can cause a series of reactions, including cell growth, proliferation and metastasis [1]. A recent study showed that Shuxuening injection induced PARs through the mTOR pathway, which is downstream of PI3K/AKT [26]. In addition, PI3K activation alters cytoskeletal mobility in Rat Basophilic Leukemia (RBL-2H3) cells, another mast cell line used in allergic reaction research [2]. Previous studies involving PI3K/AKT usually focused on the release of proinflammatory factors and cytoskeletal regulation. In this study, we found that PI3K/AKT acted downstream of MrgprX2, and regulated mast cell degranulation by increasing the intracellular Ca $^{2+}$  concentration.

The Ca $^{2+}$  signaling pathway is important for mast cell degranulation and the increase in intracellular Ca $^{2+}$  is necessary for both degranulation and cytokine release [4]. PLC- $\gamma$ , a key protein in the Ca $^{2+}$  signaling pathway, is widely expressed in many somatic cells and takes part in many physiological processes [29]. Phosphorylation of PLC- $\gamma$  was associated with increased intracellular Ca $^{2+}$  concentration in type I allergic reactions and in PARs [12,20]. In addition, some studies also showed that inhibiting the PLC- $\gamma$ /IP3 pathway also prevented mast cell degranulation. Herein, we found that C48/80 failed to induce intracellular Ca $^{2+}$  levels by following pretreatment with the PLC $\gamma$  phosphorylation inhibitor (U73122) or the Ca $^{2+}$  chelator BAPTA-AM. It is speculated that endoplasmic reticulum Ca $^{2+}$  release is an important mechanism in MrgprX2 mediated mast cell degranulation.

Interestingly, we found C48/80 could still induced a transient increase of intracellular Ca $^{2+}$  concentration in Ca $^{2+}$ -free buffer. However, when Ca $^{2+}$  was depletion by BAPTA-AM, C48/80 was no longer effective in raising Ca $^{2+}$  concentrations. Altogether, these results indicated a potential relationship between Ca $^{2+}$  release and Ca $^{2+}$  influx. This speculation was confirmed by a recent study that showed that store-

operated  $\text{Ca}^{2+}$  entry (SOCE) via the  $\text{Ca}^{2+}$  sensor, stromal interaction molecule 1 (STIM1), promotes MrgprX2-induced human mast cell response [18].

In addition to being involved in PARs, MrgprX2 takes part in promoting mast cell-dependent host defense and immune regulation, in addition to promoting the pathogenesis of pain, pruritus, and inflammatory diseases [22]. Furthermore, some studies suggest that the MAPK and NF- $\kappa$ B pathways play a role in MrgprX2-induced production and release of cytokines and chemokines from mast cells [16]. PI3K/AKT signals are upstream of the MAPK and NF- $\kappa$ B pathway. Thus, the understanding the relationship between the increased intracellular  $\text{Ca}^{2+}$  concentration induced by the activation of PI3K/AKT and PLC $\gamma$  and the above activation pathways will help to fully elucidate the mechanisms underlying MrgprX2-mediated mast cell degranulation, which may provide a direction for future research.

## 5. Conclusion

MrgprX2 is the key activator of PARs, and its activation of it results in degranulation of mast cells. Herein, we found that the PI3K/AKT signaling pathway and PLC $\gamma$  acted as downstream signals of MrgprX2 and regulated the degranulation response of mast cells by influencing intracellular  $\text{Ca}^{2+}$  concentration. These findings provide details on the underlying mechanism involved in PARs.

## Declaration of Competing Interest

The authors declare that they have no known competing financial interests or personal relationships that could have appeared to influence the work reported in this paper.

## Acknowledgements

This work was supported by the National Natural Science Foundation of the People's Republic of China, China (Grant number: 81973471 and Grant number: 81903788).

## Authors' contributions

Jin Qi and Boyang Yu designed the experiments and revised the manuscript; Fan Zhang and Fang Hong performed the experiments; Fan Zhang, Fang Hong, Lu Wang and Renjie Fu analyzed the data; Fan Zhang wrote the paper. Authorship must be limited to those who have contributed substantially to work reported.

## Appendix A. Supplementary material

Supplementary data to this article can be found online at <https://doi.org/10.1016/j.intimp.2021.108389>.

## References

- A.S. Alzahrani, PI3K/Akt/mTOR inhibitors in cancer: at the bench and bedside, *Semin. Cancer Biol.* 59 (2019) 125–132.
- M.T. Barati, J. Scherzer, R. Wu, M.J. Rane, J.B. Klein, Cytoskeletal rearrangement and Src and PI-3K-dependent Akt activation control GABA(B)R-mediated chemotaxis, *Cell. Signall.* 27 (2015) 1178–1185.
- M.D. Bootman, G. Bultynck, Fundamentals of cellular calcium signaling: a primer, *Cold Spring Harbor Perspect. Biol.* 12 (2020).
- Y.C. Chen, Y.C. Chang, H.A. Chang, Y.S. Lin, C.W. Tsao, M.R. Shen, W.T. Chiu, Differential  $\text{Ca}^{2+}$  mobilization and mast cell degranulation by Fc $\epsilon$ RI- and GPCR-mediated signaling, *CellCalcium* 67 (2017) 31–39.
- Y. Ding, Y. Wang, C. Li, Y. Zhang, S. Hu, J. Gao, R. Liu, H. An,  $\beta$ -Linolenic acid attenuates pseudo-allergic reactions by inhibiting Lyn kinase activity, *Phytother. Res.* 34 (2020) 153391.
- D.G. Ebo, J.L. Bosmans, M.M. Couttenye, W.J. Stevens, Haemodialysis-associated anaphylactic and anaphylactoid reactions, *Allergy* 61 (2006) 211–220.
- D.A. Fruman, H. Chiu, B.D. Hopkins, S. Bagrodia, L.C. Cantley, R.T. Abraham, The PI3K pathway in human disease, *Cell* 170 (2017) 605–635.
- S. Han, Y. Lv, L. Kong, D. Che, R. Liu, J. Fu, J. Cao, J. Wang, C. Wang, H. He, T. Zhang, X. Dong, L. He, Use of the relative release index for histamine in LAD2 cells to evaluate the potential anaphylactoid effects of drugs, *Sci. Rep.* 7 (2017) 13714.
- Y. Hou, D. Che, D. Wei, C. Wang, Y. Xie, K. Zhang, J. Cao, J. Fu, N. Zhou, H. He, Phenothiazine antipsychotics exhibit dual properties in pseudo-allergic reactions: activating MRGPRX2 and inhibiting the H1 receptor, *Mol. Immunol.* 111 (2019) 118–127.
- S.W. Kashem, H. Subramanian, S.J. Collington, P. Magotti, J.D. Lambris, H. Ali, G protein coupled receptor specificity for C3a and compound 48/80-induced degranulation in human mast cells: roles of Mas-related genes MrgX1 and MrgX2, *Eur. J. Pharmacol.* 668 (2011) 299–304.
- M. Kumar, K. Duraisamy, B.K. Chow, Unlocking the non-IgE-mediated pseudo-allergic reaction puzzle with mas-related G-protein coupled receptor member X2 (MRGPRX2), *Cells* 10 (2021).
- Y. Lin, J. Wang, Y. Hou, J. Fu, D. Wei, Q. Jia, Y. Lv, C. Wang, S. Han, L. He, Isosalvianolic acid C-induced pseudo-allergic reactions via the mast cell specific receptor MRGPRX2, *Int. Immunopharmacol.* 71 (2019) 22–31.
- Y. Lv, J. Fu, Q. Jia, D. Che, Y. Lin, S. Han, L. He, Accurate quantification of beta-hexosaminidase released from laboratory of allergic diseases 2 cells via liquid chromatography tandem mass spectrometry method, *J. Chromatogr. A* 1578 (2018) 106–111.
- B.D. McNeil, P. Pundir, S. Meeker, L. Han, B.J. Udem, M. Kulka, X. Dong, Identification of a mast-cell-specific receptor crucial for pseudo-allergic drug reactions, *Nature* 519 (2015) 237–241.
- A.J. Melendez, A.K. Khaw, Dichotomy of  $\text{Ca}^{2+}$  signals triggered by different phospholipid pathways in antigen stimulation of human mast cells, *J. Biol. Chem.* 277 (2002) 17255–17262.
- Y.N. Mi, N.N. Ping, Y.X. Cao, Ligands and signaling of mas-related G protein-coupled receptor-X2 in mast cell activation, *Rev. Physiol. Biochem. Pharmacol.* 179 (2021) 139–188.
- B.D. Modena, K. Dazy, A.A. White, Emerging concepts: mast cell involvement in allergic diseases, *Trans. Res.: J. Lab. Clin. Med.* 174 (2016) 98–121.
- C.J. Occhiuto, A.K. Kammala, C. Yang, R. Nellutla, M. Garcia, G. Gomez, H. Subramanian, Store-operated calcium entry via STIM1 contributes to MRGPRX2 induced mast cell functions, *Front. Immunol.* 10 (2019) 3143.
- M. Psatha, A. Koffer, M. Erent, S.E. Moss, S. Bolsover, Calmodulin spatial dynamics in RBL-2H3 mast cells, *CellCalcium* 36 (2004) 51–59.
- G.M. odrÁ-guez-LÁ<sup>3</sup>pez, R. Soria-Castro, M. Campillo-Navarro, S.M. PÁ<sup>3</sup>rez-Tapia, F. Flores-Borja, I. Wong-Baeza, S. MuÁ<sup>3</sup>oz-Cruz, R. LÁ<sup>3</sup>pez-Santiago, S. Estrada-Parra, I. Estrada-GarcÁ<sup>3</sup>a, A.D. ChÁ<sup>3</sup>vez-Blanco, R. ChacÁ<sup>3</sup>n-Salinas, The histone deacetylase inhibitor valproic acid attenuates phospholipase C $\beta$ 2 and IgE-mediated mast cell activation, *J. Leukocyte Biol.* 108 (2020) 859–866.
- A. Shiki, Y. Inoh, S. Yokawa, T. Furuno, Promotion of microtubule acetylation plays an important role in degranulation of antigen-activated mast cells, *Inflammation Res.: Official J. Eur. Histamine Res. Soc. ... [et al.]* 68 (2019) 181–184.
- H. Subramanian, K. Gupta, H. Ali, Roles of Mas-related G protein-coupled receptor X2 on mast cell-mediated host defense, pseudoallergic drug reactions, and chronic inflammatory diseases, *J. Allergy Clin. Immunol.* 138 (2016) 700–710.
- W. Sun, S. Wang, P. Liang, H. Zhou, L. Zhang, Q. Jia, J. Fu, Y. Lv, S. Han, Pseudo-allergic compounds screened from Shengmai injection by using high-expression Mas-related G protein-coupled receptor X2 cell membrane chromatography online coupled with liquid chromatography and mass spectrometry, *J. Sep. Sci.* 44 (2021) 1421–1429.
- C. Traidl-Hoffmann, Allergy - an environmental disease, *Bundesgesundheitsblatt, Gesundheitsforschung, Gesundheitsschutz* 60 (2017) 584–591.
- J. Wang, Y. Zhang, J. Wang, R. Liu, G. Zhang, K. Dong, T. Zhang, Paeoniflorin inhibits MRGPRX2-mediated pseudo-allergic reaction via calcium signaling pathway, *Phytother. Res.* PTR 34 (2020) 401–408.
- L. Wang, J. Tian, S. Liu, Y. Zhang, J. Liu, Y. Yi, C. Li, Y. Zhao, Y. Zhang, J. Han, C. Pan, G. Li, Z. Xian, A. Liang, Shuxuening injection, derived from Ginkgo biloba leaf, induced pseudo-allergic reactions through hyperactivation of mTOR, *Pharm. Biol.* 58 (2020) 581–589.
- N. Wang, R. Liu, Y. Liu, R. Zhang, L. He, Sinomenine potentiates P815 cell degranulation via upregulation of  $\text{Ca}^{2+}$  mobilization through the Lyn/PLC $\beta$ 3/IP3R pathway, *Int. J. Immunopathol. Pharmacol.* 29 (2016) 676–683.
- J.L. Weaver, M. Boyne, E. Pang, K. Chimalakonda, K.E. Howard, Nonclinical evaluation of the potential for mast cell activation by an erythropoietin analog, *Toxicol. Appl. Pharmacol.* 287 (2015) 246–252.
- M. Xu, B. Zhu, X. Cao, S. Li, D. Li, H. Zhou, V.M. Olkkonen, W. Zhong, J. Xu, D. Yan, OSBP-related protein 5L maintains intracellular IP3/Ca $^{2+}$  signaling and proliferation in T cells by facilitating PIP(2) hydrolysis, *J. Immunol. (Baltimore, Md. : 1950)* 204 (2020), 1134–1145.
- J. Ye, H. Piao, J. Jiang, G. Jin, M. Zheng, J. Yang, X. Jin, T. Sun, Y.H. Choi, L. Li, G. Yan, Polydatin inhibits mast cell-mediated allergic inflammation by targeting PI3K/Akt, MAPK, NF- $\kappa$ B and Nrf2/HO-1 pathways, *Sci. Rep.* 7 (2017) 11895.
- Z. Yi, Z. Yi, K. Huang, Y. Cao, C. Xiao, Y. Li, Q. Lu, S. Zhao, W. Luo, G. Liu, Propofol attenuates mast cell degranulation via inhibiting the miR-221/PI3K/Akt/Ca $^{2+}$  pathway, *Exp. Ther. Med.* 16 (2018) 1426–1432.
- Z. Zhao, S. Hu, P. Ma, D. Che, R. Liu, Y. Zhang, J. Wang, C. Li, Y. Ding, J. Fu, H. An, Z. Gao, T. Zhang, Neohesperidin suppresses IgE-mediated anaphylactic reactions and mast cell activation via Lyn-PLC-Ca $^{2+}$  pathway, *Phytother. Res.: PTR* 33 (2019) 2034–2043.